Tailor made synthesis of water-soluble polythiophene-graft-poly(caprolactone-block-dimethylaminoethyl methacrylate) copolymer and their {pH} tunable self-assembly and

European Polymer Journal 168 (2022) 111124

Contents lists available at ScienceDirect

European Polymer Journal

journal homepage: www.elsevier.com/locate/europolj

Tailor made synthesis of water-soluble polythiophene-*graft*-poly (caprolactone-*block*-dimethylaminoethyl methacrylate) copolymer and their pH tunable self-assembly and optoelectronic properties

Ujjal Haldar [1], Sanjoy Mondal [1], Soumyajit Hazra, Sayandeep Guin, Lamyea Yeasmin, Dhruba P. Chatterjee [2], Arun K. Nandi [*]

Polymer Science Unit, School of Materials Science, Indian Association for the Cultivation of Science, Jadavpur, Kolkata 700 032, India

ARTICLE INFO

Keywords:
Graft block copolymer
Click chemistry
Self-assembly
Optical property
Conductivity
OMEIC behavior

ABSTRACT

Here, we report a novel water-soluble polythiophene graft block copolymer i.e.; polythiophene-*graft*-poly(caprolactone-*block*-dimethylaminoethyl methacrylate)(PTh-*g*-PCL-*b*-PDMAEMA, P1) using combined polymerization techniques e.g. oxidative polymerization, ring-opening polymerization (ROP), atom-transfer radical polymerization (ATRP), and click chemistry; where π-conjugated polythiophene (PTh) is situated as the main chain and polycaprolactone-*block*-poly(dimethylamino ethyl methacrylate) remains anchored from the PTh backbone. The final polymer was characterized by ^{1}H NMR and FT-IR spectroscopy. Self-assembly behavior of the P1 polymer is investigated by high resolution-transmission electron microscopy and dynamic light scattering. Interestingly, both UV–vis and fluorescence emission peaks are shifted gently towards higher wavelength region for decreasing pH from 10 to 3, plausibly due to extension of PTh backbone caused by the repulsion of protonated –NMe_2 group of grafted PDMAEMA segment. The results show variation of nanostructures from micelle to vesicle to multivesicular assembly with the variation of pH from 3 to 7 to 10. The dc-conductivity values at pH 3, 7, 10 are 0.40 ± 0.09, 0.11 ± 0.04, and 0.12 ± 0.04 μS/cm, respectively and the highest value at pH 3 is for the uncoiled polythiophene chain arising from the ionic repulsion of protonated -$N(CH_3)_2$ group of grafted PDMAEMA block. The I-V characteristic data shows semiconducting nature with signature of organic mixed electronic and ionic conductivity (OMEIC) at pH3.

1. Introduction

The self-assembly of amphiphilic block copolymers (ABCPs) has attracted significant attention for several decades because it exhibits a wide range of ordered structures including spheres, vesicle, cylinders, bi-continuous structures, lamellae, toroidal, and many other complex or hierarchical assemblies both in the solution and in the bulk phase [1–3]. These architectures are mostly governed by hydrophobic and hydrophilic block lengths and this wide variation of morphologies of ABCPs, make them suitable for various potential applications [4,5]. Among the different block copolymer systems, block copolymers with π-conjugated segments are very useful because of their tunable optoelectronic properties, mechanical flexibility, and enhanced solubility [6–12]. These systems are broadly used in the fabrication of organic thin film transistors (OTFTs) [13], organic solar cells [14,15], organic light-emitting diodes (OLEDs) [16], and sensors [17,18]. In this regard, polythiophene (PTh) derivatives were extensively investigated among the other conjugated systems as an organic semiconducting polymer due to their outstanding physical and chemical features, solubility of its derivatives, tunable electrochemical behavior, and ease of chemical and structural modification. These outstanding features made them suitable for diverse optoelectronic applications [19].

So, the development of PTh-based graft copolymers connected with flexible, hydrophobic, hydrophilic polymer chains, have major research interest to improve the optoelectronic properties [20,21]. Over the past few years our group had synthesized a series of water-soluble PTh grafted amphiphilic copolymer consisting of various stimuli-responsive monomers such as *N, Ń*-dimethylaminoethyl methacrylate

* Corresponding author.
E-mail address: psuakn@iacs.res.in (A.K. Nandi).
[1] Equal contribution of both the authors.
[2] Department of Chemistry, Presidency University, Kolkata 700 073, India.

https://doi.org/10.1016/j.eurpolymj.2022.111124
Received 15 January 2022; Received in revised form 21 February 2022; Accepted 2 March 2022
Available online 4 March 2022

(DMAEMA), uracil etc. using combination of electron transfer polymerization (ETP) and atom-transfer radical polymerization (ATRP) techniques [22,23]. Recently, Alemán and his research group synthesized PTh-based polymer with poly(ethylene glycol, PEG) or polycaprolactone (PCL) side chains via electrochemical copolymerization technique, and successfully revealed bioactive cellular matrices and electroactive bioadhesive surfaces pertinent for biomedical and biotechnological applications [24,25]. The same group has recently developed a new heterografted rod-coil statistical copolymer, having π-conjugated PTh main chain and polar polyethylene glycol (PEG_{2000}) and oligo-caprolactone side chains showing two different types of supra molecular structures e.g. porous spherical particles and rod-like structures [26].

On the other hand, stimuli-responsive polymers with environmental sensitivities (such as pH, temperature, light, redox, voltage, ions, etc.) have earned significant research attention over the last few decades for their various potential applications particularly in sustain drug-delivery and other similar applications [27–29]. Among the various stimuli, pH is the most significant chemical stimuli not only, for its inherent chemical features to make easily tunable systems but also, for its enormous role to control the self-assembly of various nanostructures, control drug delivery, solar cell, sensing, etc. [30–32]. Due to such novelty, scientists are engaged in synthesizing different pH responsive copolymer, block copolymer, and graft copolymers for specific purposes. Among the different systems, pH-responsive polythiophene block copolymers are quite interesting as it can tune the self-assembly by manipulating the hydrophobic and/or hydrophilic blocks influencing the opto-electronic properties. Several poly(3-alkyl thiophene)(P3AT) -based rod–coil block copolymers were synthesized for different optoelectronic applications [33–35] but, report on PTh grafted pH-responsive block copolymer is comparatively low [18,19,24]. Chen et al reported nitroxy mediated polymerization of styrene from poly(3-hexyl thiophene) and then reacted with C_{60} to yield a soluble graft, rod-coil polymer. The polymer films displayed a bi-continuous phase structure and showed good optical properties for extensive *π*-delocalization [36]. Therefore, it would be really exciting to synthesize polythiophene graft block copolymer with hydrophobic and hydrophilic blocks and to examine the overall self-assembly and optoelectronic properties in aqueous media.

Considering these facts in mind, we have synthesized a novel hetero grafted block copolymer of π-conjugated PTh main chain where PCL and PDMAEMA blocks remain anchored as the side chain of the copolymer (PTh-*g*-PCL-*b*-PDMAEMA) (P1). Here both PTh and PCL blocks are hydrophobic in nature and PDMAEMA block acts as hydrophilic unit showing pH sensitivity via protonation/deprotonation of its $-N(CH_3)_2$ group. Thus interesting pH sensitive self-assembly and optoelectronic properties of the P1 in aqueous medium is expected. Amazingly, the self-assembling behavior of P1, examined by HRTEM study at various pH, indicates that at pH 3 it adopts micellar structure but at pH 7 the P1 block-copolymer takes the shape of a vesicle and at pH-10 multi-vesicular aggregates are produced. The UV–vis and fluorescence peaks show a gentle shift towards higher wavelength on decreasing the pH from 10 to 3, probably due to uncoiling of the polythiophene chain caused by the repulsion of protonated $—NMe_2$ group of grafted PDMAEMA block. This induces dc-conductivity values of P1 films to increase at lower pHs and also influences the current-voltage (I-V) characteristic data. At pH7 the I-V data exhibit purely semiconducting nature but at pH3, an interesting organic mixed electronic and ionic conductivity (OMEIC) nature is noticed arising from the conductivity of protons at higher voltage apart from the electronic conductivity of the PTh main chain.

2. Experimental

2.1. Materials

Prior to the polymerization, the monomer *N, Ń* dimethylaminoethyl methacrylate (DMAEMA) were passed through a small plugged basic alumina column to remove the ppm level of free radical inhibitor. Caprolactone monomer (Sigma Aldrich) was used as received. Cuprous chloride was purchased from Sigma Aldrich and was purified as mentioned in literature [22,23]. The solvents such as *N*, *Ń* dimethyl formamide, diethyl ether, anisole, dichloromethane (DCM), chloroform, methanol, hexanes (mixture of isomers) were purified by distillation. NMR solvent, $CDCl_3$ (99.8% D) was purchased from Sigma and was used for ^1H NMR spectroscopic investigations. All other reagents of the highest purity were obtained from commercial sources, and were used as received without any further purification. De-ionized distilled water was used for the preparation of different pH solutions.

2.2. Synthesis of compound 1

Hydroxyl end of thiophene moiety at 3-position was tosylated using one step nucleophilic substitution reaction with tosyl chloride in the presence of triethyl amine in DCM (Scheme-1). The compound was synthesized according to the earlier literature reports [37]. The observed NMR (Fig. S1a,b,c) data was nicely matched with the reported values. The ^1H NMR data (Fig. S1a,b, 500 MHz, in $CDCl_3$) involved characteristic chemical shifts at δ (ppm): 6.96 (—SC***H***═C—,1H, s, peak a), 7.21 (—SC***H***═C—, 1H, s, peak b), 6.86 (—SCH═C***H***—, 1H, d, peak c), 2.97 (—O—CH_2—C***H***$_2$—, 2H, t, peak d), 4.21 ((—O—C***H***$_2$—CH_2—, 2H, t, peak e), 7.71 (phenyl protons, 2H, dd, peak f), 7.32 (phenyl protons, 2H, dd, peak g), and 2.44 (—C***H***$_3$—, 3H, s, peak h). The ^{13}C NMR peaks are assigned in Fig. S1c; *δ* (ppm): 144.84, 136.54, 133.15, 129.69, 127.99, 127.14, 122.24, 70.06, 29.94, 21.55, 14.24.

2.3. Synthesis of compound 2

Prior to the insertion of $FeCl_3$ into the round bottom (250 ml) single necked flask, dry N_2 was flushed into it for 10 min to make the system inert. Then, anhydrous fresh $FeCl_3$ (15 mmol) was dispersed in 30 ml dry chloroform and was transferred to the flask. The compound 1 (3.5 mmol in 30 ml of dry chloroform) was added at a time into the reaction mixture and was stirred overnight at 20 °C. After predetermined time, the reaction mixtures were added into the excess amount of methanol with continuous stirring. The solid precipitate was separated, washed with excess methanol repeatedly and finally it was soxhlet extracted with methanol followed by DCM. The extract was dried under high vacuum at 40 °C for 12 h. A red colored solid was obtained as a final product (yield: ~85%). The corresponding NMR spectra of the compound 2 was depicted in Fig. S2.

2.4. Synthesis of Poly(A)

Azide end-linked polythiophene was obtained via one step bimolecular nucleophilic substitution reaction. Typically, Compound 2 (100 mg) was dissolved in 3 ml anhydrous DMF in 20 ml septa sealed polymerization vial equipped with a small magnetic bead and was stirred at room temperature. To the stirred solution, sodium azide (~10 times excess with respect to compound 2) was added instantly and was stirred for further 24 h at the same temperature. Finally, the polymer was precipitated twice with excess amount of methanol. The purity of the compound was judged by ^1H NMR spectra (Fig. 1a). FT-IR spectra is carried out for poly(A) (Fig. S3), and a sharp absorption streching fequency at 2100 cm^{-1} indicate presence of azide group.

2.5. Synthesis of compound 3

Alkyne-terminated oligo-caprolactone (Alkyne-PCL) macromonomer was synthesized using metal catalyzed ring-opening polymerization techniques. Typically, 0.02 g of 3-butyn-1-ol and 4.0 ml caprolactone (CL) were taken in a 40-mL septum-sealed polymerization vial. Then, catalytic amount of $Sn(Oct)_2$ (1 ml) was injected into the vial under N_2 atmosphere. The sealed vial was immediately placed in a preheated oil

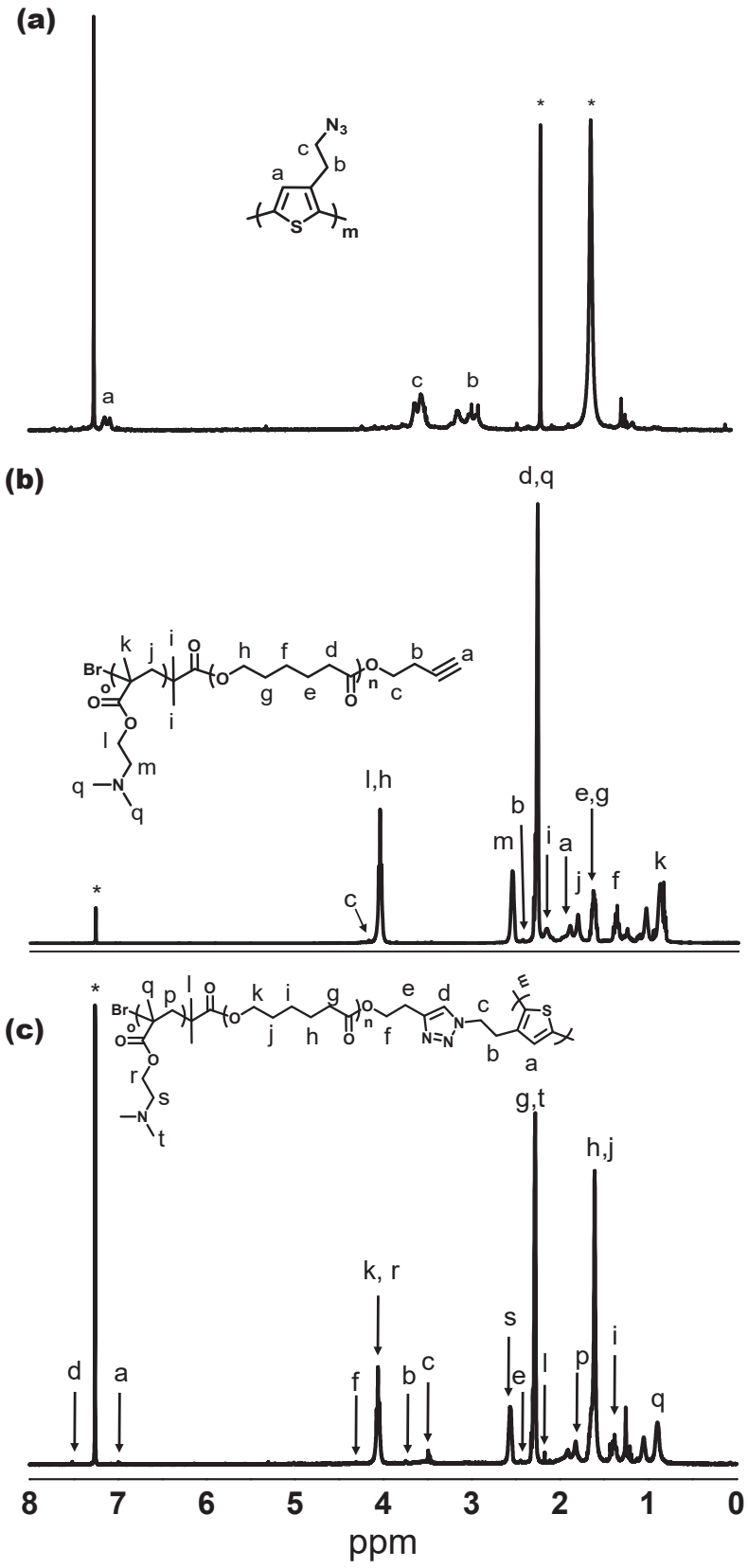

Fig. 1. ^{1}H NMR spectrum of compound (a) **Poly(A)** (b) **Poly(B)** and (c) **P1** in $CDCl_3$. Asterisk may indicate trapped solvent resonance.

bath at 90 °C. After 10 h, the vial was cooled to room temperature. Finally, the viscous product was diluted with DCM and was precipitated in cold diethyl ether (3 times). The final product was dried under vacuum at 30 °C for 24 h. The purity of the polymer and the chain-end of the polymer was nicely depicted in ^{1}H and ^{13}C NMR spectra shown in Fig. S4 (a-c) and the ^{1}H NMR peak position at ~2 ppm (Fig. S4a,b) supports the *yne* terminated polycaprolactone (PCL) formation and the ^{13}C NMR spectra (Fig. S4c) also demonstrate the sharp peak at ~77 ppm for *yne* carbons in compound 3.

2.6. Synthesis of compound 4

Typically, compound 3 (1 gm) was dissolved in dry DCM (30 ml) in a 100 ml round-bottom flask. Then, triethylamine (1.5 equivalent with respect to compound 3) was added into the reaction mixture and was stirred continuously at 0 °C under nitrogen atmosphere. 2-bromoisobutyryl bromide (BIB, 1.2 mmol), diluted with 10 ml dry DCM, was added into the reaction mixture drop wise using a pressure-equalizer and was stirred for 24 hrs. Finally, the polymer was precipitated with cold diethyl ether (twice) to get a light-yellow solid polymer. The formation of the Compound 4 was confirmed by ^{1}H NMR spectroscopy (Fig. S5).

2.7. Synthesis of Poly(B)

Compound 4 (25 mg), anisole (2 ml), CuBr (10 mg) were taken in a N_2 purged reaction vessel (8 × 2.5 cm). The monomers DMAEMA (1.0 ml) were then injected into the reaction tube under nitrogen purged condition. The ligand HMTETA (30 μL) was finally inserted into the reaction mixture and the reaction was allowed to stir for 12 h at 80 °C. The reaction mixture was then precipitated into the excess petroleum ether. The precipitated polymer was isolated, re-dissolved in THF and was re-precipitated into excess petroleum ether. This process was repeated for three times to remove any trace amount of monomer entrapped within the polymer. Then the polymer was dissolved in THF and was passed though silica column to remove the copper catalyst. Finally, by evaporating the solvent, the alkyne terminated PCL-b-PDEMAEMA polymer was obtained (Fig. 1b).

2.8. Synthesis of polymer (polythiophene-graft- PCL-b-PDMAEMA, P1)

To obtain the target final polymer, P1, Poly(A) was coupled with Poly(B) using a well-known copper catalyzed click reaction [38]. In a 20 ml septa-sealed polymerization vial, both the pre-polymer was dissolved in 4 ml anhydrous THF. Then, the catalytic amount of CuBr and HMTETA ligand was added under an inert atmosphere and was stirred for 24 h at room temperature. Finally, the target polymer was collected after removing the Cu metal by passing it through small plugged basic alumina column. After getting the final polymer, it was further precipitated by cold hexane (twice). The resulting polymer was dried under room temperature and was characterized thoroughly using NMR spectroscopy (Fig. 1c). The peak at δ 7.5 (peak d) ppm was assigned to the hydrogen atoms present in the 5-membered triazole ring formed by the azide-alkyne click reaction of poly A and poly B. This is also supported from the absence of 2100 cm^{-1} FTIR peak of poly(A) in FTIR spectrum of P1 (Fig. S6).

2.9. Instrumentation

The characterization of the monomer, pre-polymers, and final polymers were monitored by various spectroscopic tools. The details of these instruments are systematically described below.

2.10. ^{1}H NMR spectra

The ^{1}H NMR (^{1}H nuclear magnetic resonance) study was conducted using 500 MHz Bruker instrument.^{13}C NMR Spectra was carried out in 400 MHz Bruker NMR instrument. $CDCl_3$ was used as NMR solvent and tetramethylsilane (TMS) was used as an internal standard. The measurement was carried out at 298 K.

2.11. UV–vis and photoluminescence (PL) Spectroscopy

The UV–vis and photoluminescence (PL) spectra of the samples were studied using a UV–vis spectrophotometer (Hewlett-Packard, model 8453) and Fluoromax-3 instrument (Horiva Jovin Yvon), respectively. Both the measurements were carried out at 30 °C using solutions at different pH. For PL measurement, the sample was excited at 415 nm and the emission scans were recorded from 440 to 800 nm using a slit width of 1.5 nm with an increment of 1 nm wavelength having an integration time of 0.1 s.

2.12. Fourier Transform Infrared Spectroscopy (FTIR)

The FTIR spectra of all the solid samples were performed in a Shimadzu FTIR instrument (model 8400S) from KBr pellets. Whereas, the liquid samples were carried out in dedicated IR plate.

2.13. Dynamic Light Scattering (DLS)

The DLS experiments of the P1 polymer solutions (0.10% w/v) at three different pHs were performed using a Malvern instrument with a He-Ne laser at an angle 173° at 25 °C. To measure the surface charge, the zeta potential values of the aqueous solution of polymer samples (0.15% w/v) were measured using the same DLS instrument at 25 °C at different pH.

2.14. Transmission Electron Microscopy (TEM)

Various nanostructures of polymer samples at different pH values were monitored by HRTEM instrument (JEOL, 2010EX) operated at an acceleration voltage of 200 kV fitted with a CCD camera. Polymer solutions at different pH were gently deposited on a carbon-coated copper grid via drop casting method, dried in air at 30 °C and was finally preserved at vacuum for 1 day before the TEM analysis.

2.15. Conductivity and current -voltage (I-V) measurements

The DC conductivity were measured with Keithley source meter (model 2410) using films casted from solutions at different pH on ITO strip and was sandwiched with another ITO electrode. The lower pH is made from HCl solution, pH 7 is made from distilled water and the higher pH is made from NH_4OH solution monitoring from a pH meter. For both the conductivity and I-V measurement the films were dried after keeping in vacuum for 2 days at 30 °C to eliminate any moisture effect.

3. Result and discussion

The detailed synthetic route for the preparation of polythiophene-*graft*-poly(caprolactone-*block*-dimethylaminoethyl methacrylate) (i.e.; PTh-*g*-(PCL-*b*-DMAEMA)) copolymer, named P1, is depicted in scheme 1. To obtain the target desired polymer **P1**, a couple of polymerization methods along with click chemistry are adopted. Initially, hydroxyl group at 3-position of thiophene moiety is transformed into tosyl group in the presence of slight excess of tosyl chloride and Et_3N in dry DCM, yielding compound **1**. To confirm the purity of the compound **1**, ^{1}H NMR (Fig. S1a,b) and ^{13}C NMR (Fig. S1c) experiments were conducted. All the characteristic proton and ^{13}C NMR signals, marked on the structure of compound 1 are assigned in Fig. S1(a,b,c). Then, tosyl linked thiophene unit is oxidatively polymerized with anhydrous ferric chloride ($FeCl_3$) initiator in dry chloroform. The yield of the polythiophene (PTh) homopolymer (named compound **2**) was quantitative (yield: 90%) and

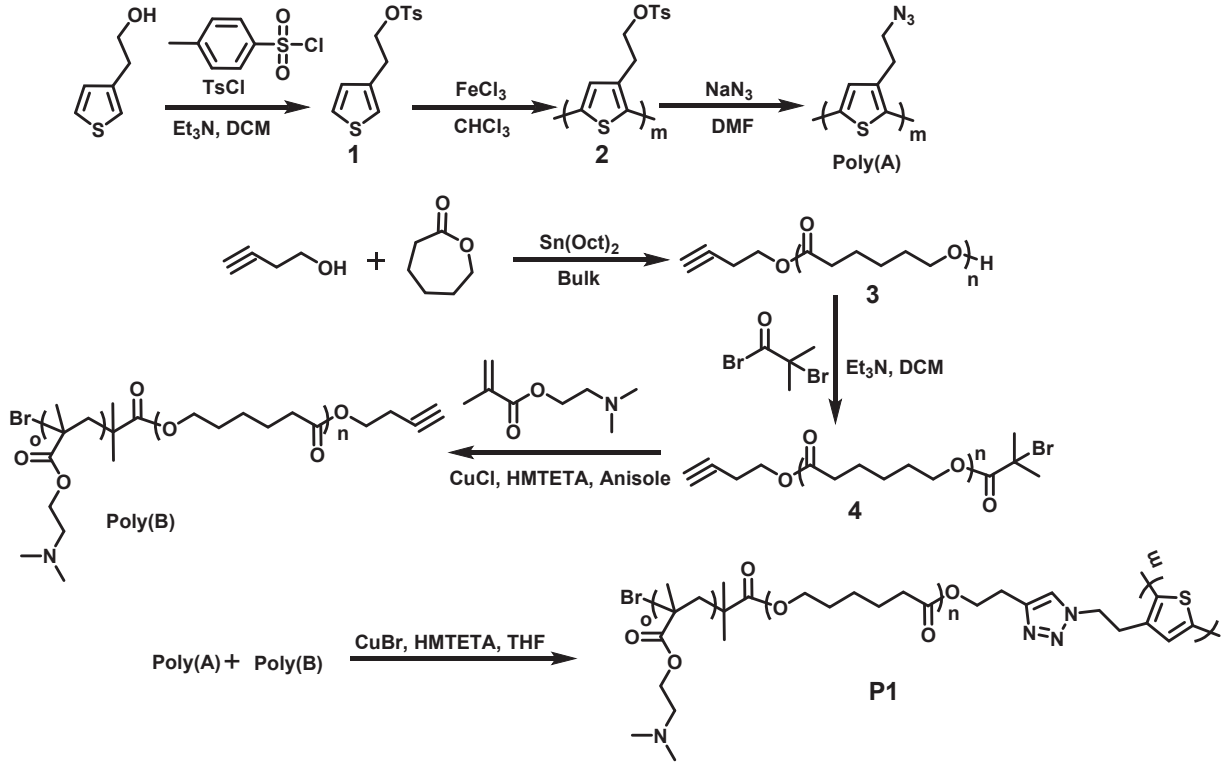

Scheme 1. The detail synthetic route of P1.

carries tosyl group at every thiophene segments. To assure the successful formation of compound **2**, ^{1}H NMR study was carried out. It was found that, NMR signals of compound **2** becomes broadened compared to those of thiophene derivative, suggesting the polymer formation and all the characteristic signals of compound **2** are assigned in Fig. S2. Interestingly, the peak position at b and c appearing at the region ~3–4 ppm exhibits clear splitting due to the presence of regio-irregularity in the linkages (head–head, H-H and tail– tail, T-T) of the thiophene moieties in the polythiophene backbone of compound 2 [39–41]. The signals at ~3.75 ppm and ~3.25 ppm may be attributed to the '$b_{H\text{-}T}$' and '$b_{H\text{-}H}$' respectively [40,41]. The degree of regio-irregularity is therefore measured from the signal area ratio of these two methylene signals which gives H-T regioregularity of polythiophene chains with about 32% abundance. So there is large amount of stereo regioirregularity (~68%) and the reason for such large amount of regioirregularity in polythiophene backbone is unknown. Probably it may arise from the bulkier tosyl side chain that may hinder the formation of regioregular H-T linkages in the polymer.

Then, the tosyl group of PTh is converted into the azide groups in presence of excess amount of sodium azide in anhydrous DMF, leading to the formation of PTh-N_3 (named PolyA). Notably, tosyl proton signals appearing at the aromatic region of compund **2** (Fig. S2) completely disapper as evident from the NMR spectrum (Fig. 1a), indicating the successful formation of Poly(A). For further confirmation, FT-IR measuement (Fig. S3) is carried out, and a sharp absorption streching fequency at 2100 cm^{-1} appears due to the vibraton band of azide functionality.

Once we have azide terminated PTh in our hand, we have synthesized alkyne terminated polycaprolactone-block-polydimethyl aminomethacrylate via dual controlled polymerization techniques i.e.; ring-opening polymerization (ROP) followed by atom-transfer radical polymerization (ATRP) under ambient reacton condition. Firstly, ROP of caprolactone was carried out in the presence of 3-butyn-1-ol as an initiator and $Sn(Oct)_2$ as heterogeneous catalyst at 70 °C with the concentration ratio [monomer]/[initiator] = 25. To know the strucrual purity, ^{1}H NMR spectroscopy was carried out, and it was found that all the important signals belonging to PCL units are clearly visualised and are assigned nicely (Fig. S4a,b). The acetylene protons appears at (2.02 ppm, peak i) and ^{13}C NMR spectra (Fig. S4c) shows a sharp peak at ~77 ppm for *yne* carbons in compound 3. The intregal ratio of acetylne proton at (2.02 ppm, peak i) and methylene protons next to ester functionality (2.25–2.32 ppm, peak f) help us to calculate the degree of polymerization (DP) of the resulting polymer and the obtained DP is about18.

In the next step, the free hydroxy end of alkyne terminated PCL was reacted with α-bromo isobutyryl bromide (ATRP initiator) in the presence of Et_3N. It was noticed that, NMR signal of methylene proton next to hydroxyl end of former polymer has shifted to lower field region after functionilzation with ATRP intiator, indicating the successful synthesis of compound 4 (Fig. S5). Then, the compound 4, having the alkyne group at one end and ATRP initiator on the other end, is employed as macro-initiator for the ATRP polymerization of DEMAEMA in the presence of HMTETA and CuCl, which acts as a ligand and catalyst for the polymerization. ^{1}H NMR spectrum shows NMR signals belonging to both the PCL and PDMAEMA, and are nicely assigned in Fig. 1(b). To determine the DP of PDMAEMA block, the proton NMR signals of methylene protons of PCL (intregated area of peak e & g) was compared with the pronton NMR signal of –$N(Me)_2$ protons appearing at 2.24 ppm. The calculated DP of PDMAEMA units of poly(B) was found around 33.

Finaly, poly(B) having free alkyne end was coupled with poly(A) using well-known click chemistry with CuBr as catalyst and HMTETA as ligand [38], resulting the target polymer polythiophene-*graft*-poly(caprolactone-*block*-dimethylaminoethyl methacrylate) PTh-*g*-(PCL-*b*-DMAEMA) copolymer; P1. The resulting polymer, P1, was thoroughly characterized by ^{1}H NMR spectroscopy. All the proton NMR signals belonging to PTh, PCL, and PDMAEMA were nicely assigned in Fig. 1c. The important signals of triazole ring (resulting from the alkyne azide click reaction) at 7.45 ppm strongly suggest the successful grafting by click reaction. Furthermore, we did not find the free alkyne and azide part, which also assure us the coupling reaction was pretty quantitative.

Additionally, the FTIR spectrum (Fig. S6) of the final polymer P1 indicates the complete absence of azide vibration peak at 2100 cm^{-1} of Poly A supporting the complete transformation of Poly A into P1 via click reaction with Poly B.

3.1. Morphology

The HRTEM images of P1 at different pHs are presented in Fig. 2 and it is evident from Fig. 2a that at pH-3 in each object there is black core and a corona surrounding it indicating the micelle formation. The black core is produced from π-stacked polythiohene backbone along with hydrophobic PCL blocks while the surrounding corona is produced from the PDMAEMA block with protonated side chains formed from dimethyl amino group at this acidic pH facilitating to remain solvated by surrounding water dipoles. Columbic repulsion between the positively charged dimethyl amino groups solvated in aqueous medium cause spreading of it surrounding the black core producing the corona of micellar structure. To prove this assertion a comparison of EDX analysis at the core and surface of the micelle (Fig. S7a,7b) is made indicating higher amount of sulphur (5.07 atom%) at the core than at the surface (4.49 atom%) and higher amount of nitrogen (1.97 atom%) at the surface than that at the core (1.00%). A slightly higher amount of oxygen percentage (0.6 atom%) at the surface than that of the core may arise from carboxyl oxygens of PDMAEMA block present in the corona of micellar structure. This proves that the black core is produced from π-stacked polythiophene backbone along with the hydrophobic PCL blocks while the surrounding corona is produced from the PDMAEMA block with protonated side chains formed from dimethyl amino group at this acidic pH. However, it may be noted that there are objects with two different contrast in Fig. 2a and it may arise for objects present in multiple layers; the upper part becomes well focused whereas the lower part is in somewhat off-focused state. Certainly, the images in Fig. 2a and b has some difference. A careful look on the objects in Fig. 2b indicates that at the centre there is a blank space surrounded by a black border in most of the objects and this is characteristics of vesicular morphology. The central blank space, filled by solvated water during its formation, became empty when dried to deposit onto the TEM grid and the surrounding black part arises from the aggregated hyrophobic polythiophene and polycaprolactone chain along with the collapsed PDMAEMA unit at this pH (pH-7). At this pH the collapsing of pendent unprotonated dimethyl amino group to the hyrophobic polythiophene backbone and polycaprolactone block occurs holding some water molecules adhered to the -$N(CH_3)_2$ group with water dipoles for solvation; thus water molecules remain entrapped and on drying the central blank space is produced. The inset image in Fig. 2b is the image of an object observed at a part of the same TEM grid at higher magnification clearly demonstrating the representative of a vesicle formed in P1 at pH7.

At pH-10 (Fig. 2c), these vesicles tend to aggregate as the outer grafted chains totally collapse producing the multi-vesicular aggregates. This is because at the centre of each vesicle of the aggregate blank space is noticed and this aggregation occurs, as there is practically no charge remains (cf. Fig. 3d) for interaction of the collapsed grafted PDMAEMA chains with water dipoles, facilitating vesicle surfaces to overlap through π-stacking and hydrophobic interactions causing the multi-vesicular assembly formation. The average diameter of P1 at pH = 3, 7 and 10, measured from the TEM images, are 42 ± 8, 63 ± 15 and 111 ± 25 nm, respectively and this increase may be attributed to the aggregation of particles with increase of pH due to collapsing of the grafted chains with increase of pH.

From the DLS plots (Fig. 3a-c) it is evident that there is also an increase of hydrodynamic diameter from 50 nm at pH3 to 69 nm at pH7 and reaches to 164 nm at pH10. This increase is similarly attributed to the aggregation of particles with increase of pH and the sizes are higher than the respective average TEM sizes, as expected due to solvation of the particles in the solution state. This increase of sizes with increase of pH is caused from the decrease of positive charges (cf. Fig. 3d) facilitating better aggregation of polymer particles thus increasing the hydrodynamic volume. The decrease of positive charges with increase of pH is very much evident from the decrease of zeta potential with increase of pH (Fig. 3d) and the charge is almost zero at pH10. This supports the above explanation of morphology transformation from micelle to vesicle to multivesicular aggregate. At pH 3, the DLS data of PI in aqueous medium indicate that the hydrodynamic size is 7 nm larger than the TEM size and this is similar to that of pH7. As DLS data are measured in aqueous media so there reside some immobilized water due to solvation both at the surface and also at the interior of the particles. In case of pH3 it may be called as 'swollen' micelles and the hydrodynamic size is larger by 8 nm from the average TEM size. In case of pH7 the vesicles also get solvated at the surfaces increasing the size. The hydrodynamic volume of PI at pH10 is relatively higher (53 nm) than the average TEM size and it may arise for the solvation of aggregated vesicles where solvation is relatively larger compared to others because of solvation of each vesicle to produce the multivesicular self-assembly.

3.2. Optical property

The UV–vis spectra of the grafted block copolymer P1 at pH 3,7 and 10 are presented in Fig. 4a and it is evident from the Fig. 4 that the π-π* transition of the conjugated polythiophene chains appear at 400 nm at pH = 3 and this peak becomes blue shifted to 395 nm at pH = 7 and pH = 10. This is because at lower pH (pH = 3) the polythiophene main chain of P1 remains more extended than that at pH 7 and pH10, due to repulsion between protonated grafted PDMAEMA chains of P1, thus increasing the conjugation length causing lower band gap. The fluorescence spectra of P1 (Fig. 4b) also exhibit similar blue shift of the emission peak from 575 nm at pH = 3 to 566 nm with increasing pH to

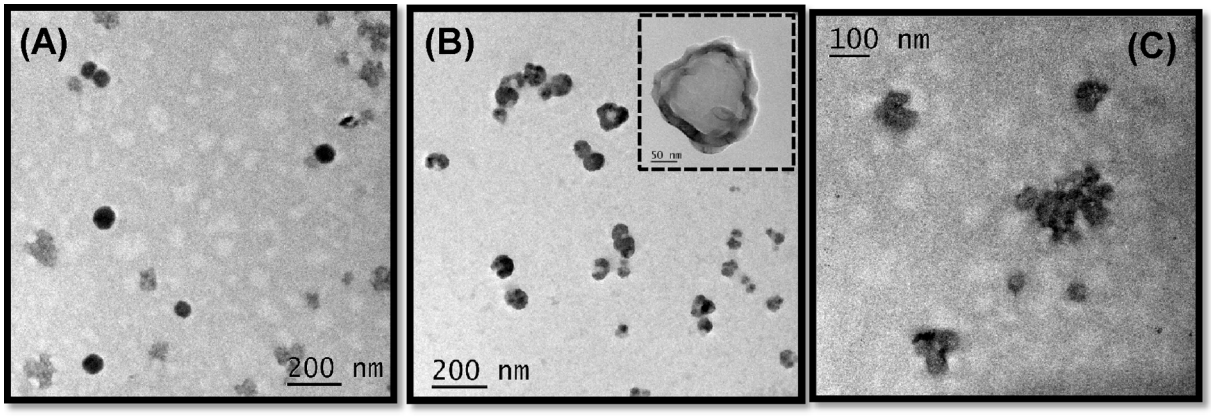

Fig. 2. HRTEM images of P1 at (a) pH3, (b) pH7 and (c) at pH10.

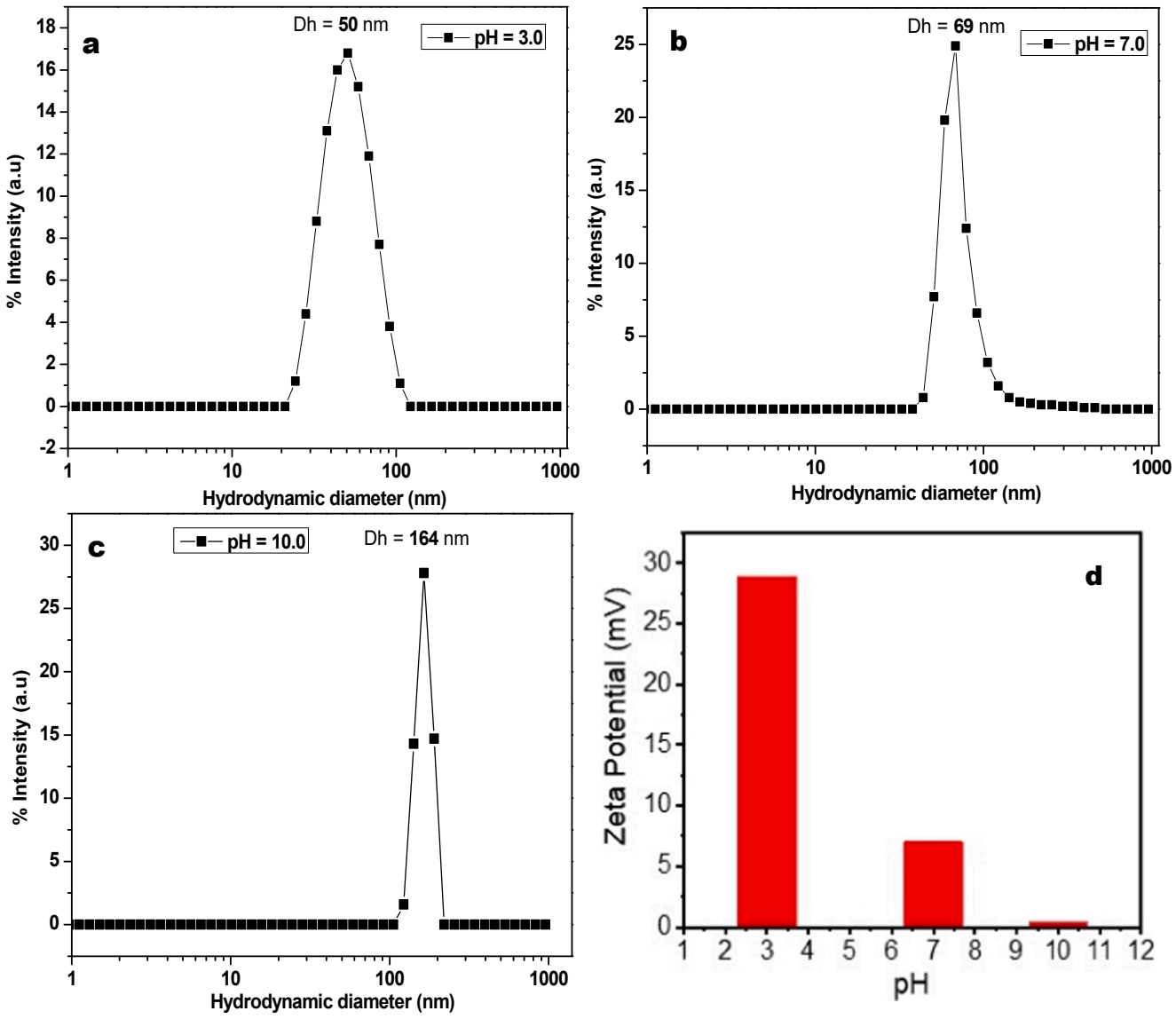

Fig. 3. DLS plot of P1 (a) at pH 3, (b) at pH 7, (c) at pH 10, and (d) Zeta potential of P1 at different pH.

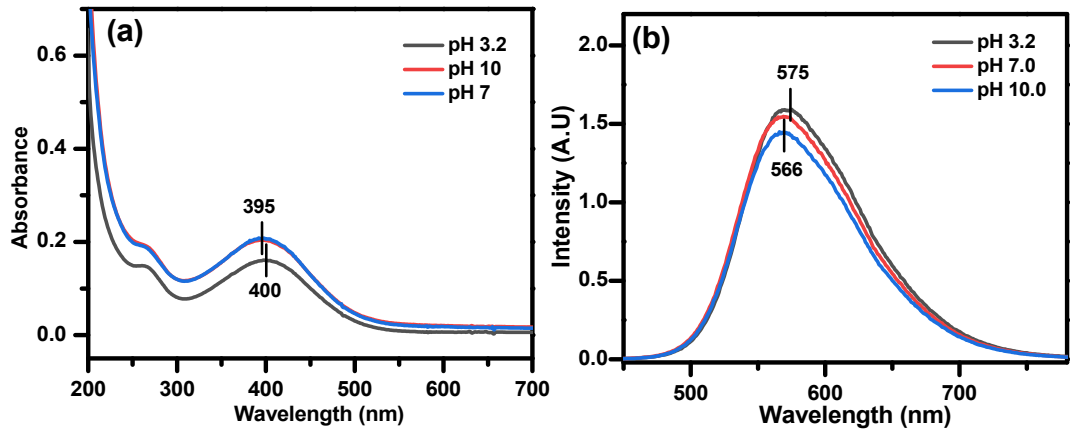

Fig. 4. (a) UV–vis, and (b) FL emission spectra of P1 at pH 3, 7, and 10 respectively. Concentration of the polymer was 10^{-4} M.

pH 7 and pH10. This is due to the fact that at pH3 the comparatively longer extended chain of polythiophene has lower band gap thus emitting lower energy (higher wavelength) than that at pH 7 and 10. Also, there is some decrease in PL- intensity with gradual increase of pH and it may be attributed to the aggregation induced quenching at these higher pH values.

3.3. Conductivity

The dc -conductivity values of P1 films casted at pH 3, 7 and pH 10, measured by two probe method, are 0.40 ± 0.09, 0.11 ± 0.04, and 0.12 ± 0.04 μS/cm, respectively indicating the semiconducting nature of the samples. The statistical analysis of dc-conductivity measurement for 10 different experiments of all three pHs is also presented in Fig. S8. The dc-conductivity values of these samples may be attributed to the flow of electrons along the polythiophene backbone [42]. Actually oxidative polymerization of compound 1(scheme-1) using $FeCl_3$ in 1:4 mol ratio may result in doping by residual $FeCl_3$ [43] and evidence of radical molecular cations present in polythiophenes made by oxidative polymerization with $FeCl_3$ was also previously reported from MALDI mass experiment [44]. This may be the reason for the generation of electronic conductivity in the P1 graft copolymer. At pH-3 dc-conductivity of P1 is ~4 times higher from that of neutral pH (pH-7) indicating that the acid in pH3 is helping in protonation which may be termed as secondary doping. The protonation of the -$N(CH_3)_2$ groups of PDMAEMA block of P1 graft copolymer makes positively charged —$NH^+(CH_3)_2$ groups. These charged pendent groups repel each other causing the PTh chain more uncoiled which increases it's conjugation length resulting in four times increase of dc- conductivity. In case of pH10 the slight higher dc-conductivity than that of pH-7 may arise for the aggregated vesicular morphology where delocalization of π electrons increases slightly due to overlapping of PT chains.

3.4. Current (I)-Voltage (V) property

The pH dependent current (I)-voltage (V) property of polythiophene-graft- PCL-b-PDMAEMA, (P1) films casted at different pHs (Fig. 5 and Fig. S9) is very interesting. In all pHs (pH = 3,7,10), the I-V curves of P1 shows semiconducting nature and at pH7 (inset of Fig. 5 and Fig. S9) the P1 shows purely electronic conductivity arising from the conjugated backbone of polythiophene showing the lowest current at each voltage compared to those of other pHs. At pH 3 the -$N(CH_3)_2$ group of PDMAEMA becomes protonated with H^+ ion which increases the electronic conductivity by uncoiling of conducting P3HT chain due to repulsion between positive charges. It also promotes ionic conductivity, possibly by the interchain hopping of protons [45,46] which increases through the protonated -$N(CH_3)_2$ groups of PDMAEMA blocks with increase of voltage showing the maximum conductivity of 1.4×10^{-3} A at +5 Volt. A comparison of conductivity values at +5 V of P1 at pH3 and that at pH7 indicates about four orders increase of conductivity due to contribution of mostly ionic conductivity arising from the hopping of protons and it is also true for the negative bias. A careful look on the I-V plot of pH3 indicates that at the initial voltage range (−1.5 to +1.5 V) the current is nonvariant, then with an increase of voltage, P1 shows a sharper increase of current than the I-V plots of pH 7 at both positive and negative bias. This is quite an interesting phenomenon and it may arise for the greater flow of charges along the PT chain indicating that it almost behaves like a diode. This type of I-V plot resembles to that in the blends of polymer electrolytes with conjugated polymers where the movement of ions of the electrolyte causes sharp hike in conductivity [47]. It is also observed in the poly(3-thiophene acetic acid)–NaDNA hybrid where Na+/ H+ possibly contributes to the sharp hike of conductivity[48] at the higher voltages. Similar type of I-V curve is also recently noticed by us in a polymer-peptide conjugate where the contribution of both electronic and ionic conductivity of iodide ions of the cationic polythiophene have been established [42]. Thus the present system is a good example of organic mixed ionic–electronic conductors (OMIECs) [49–51], where both the electronic and ionic conductivity contribute to the I–V plot. At pH-3 the —$N(CH_3)_2$ group of P1 got protonated which may result in the generation of ionic conductivity and it increases with increase of voltage through proton hopping mechanism [45,46] and the electronic conductivity arises from the flow of electrons through the conjugated polythiophene chain. This OMEIC property present in the polymer P1 is very interesting for the development of next-generation bio-electronic, opto-electronic and energy storage devices [50,51]. At pH 10, P1 also shows an initial nonvariant I-V plot, then it increases sharply with increase of voltage and the conductivity at +5 V (~1.2×10^{-7} A) is two times higher than the conductivity (electronic) of pH7 (0.6×10^{-7} A) at +5 V. This two-times higher conductivity arises due to ionic contribution and possibly during drying of the ammonium hydroxide, used to make pH10, few NH_4^+ ions remain entrapped at —$N(CH_3)_2$ centers via co-ordination and contributes to the ionic conductivity at +5 V. Thus at pH10, P1 is also showing some OMEIC characteristics but it is lower than that of pH3. The bulkier size of ammonium ion experiences some restricted mobility [45,52] with increase of voltage compared to that of H^+ in pH3, so contribution of ionic conductivity is lower at this pH compared to that at pH3. Also at pH10 there is a signature of rectification property (rectification ratio = 1.4). The small rectification ratio arises here due to *p/n* junction formation from the intimate mixing of the trapped charges on the surface of aggregated vesicles.

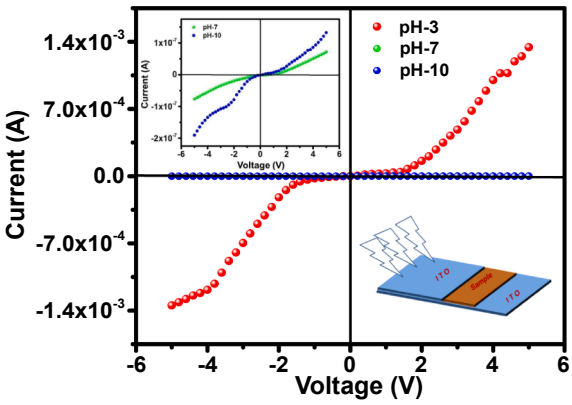

Fig. 5. I-V plot of polythiophene-graft- PCL-b-PDMAEMA at different pH.

4. Conclusion

So we have been able to make a tailor made synthesis of PTh-g- (PCL-b-PDMAEMA), (P1) using combined polymerization techniques such as oxidative polymerization, ring-opening polymerization (ROP), click chemistry and atom-transfer radical polymerization (ATRP), with π-conjugated polythiophene chain as the backbone and PCL-b-PDMAEMA as the grafted chain. The polymer is characterized well by ^1H NMR spectra and has the composition PTh-g-PCL_{18} -b-$PDMAEMA_{33}$. The graft copolymer is water soluble, highly pH-responsive and shows pH- dependent aggregation showing micelle to vesicle to multivesicular aggregate formation with increase of pH from 3 to7 to10. The change in particle size arising from the self assembly is also evident from DLS study and the Zeta potential plot with pH shows a clear decrease of positive charge with increase of pH. Both UV–vis and fluorescence spectra shows gentle blue shift in their respective peak positions with increase of pH due to coiling of polythiophene main chain with increase of pH. The dc -conductivity values of P1 film at pH3 is ~4 times higher than that of pH7 and the I-V curve clearly indicates the property of organic mixed electronic and ionic conductivity (OMEIC) at pH3 but it is absent at pH7. The OMEIC behavior has been attributed to the protonation of -$N(CH_3)_2$ group contributing to the ionic conductivity apart from the electronic conductivity of the main PTh chain. The OMEIC property in the present system is very interesting for the development of next-generation bio-electronic, opto-electronic and energy storage devices.

Declaration of Competing Interest

The authors declare that they have no known competing financial

interests or personal relationships that could have appeared to influence the work reported in this paper.

Acknowledgements

We gratefully acknowledge CSIR, New Delhi (ES grant (21(1055)/18-EMR-II)) for financial support. S.H acknowledges UGC, New Delhi for the fellowship.

Appendix A. Supplementary material

NMR Spectra of compound **1,** compound **2,** compound **3,** compound **4** of scheme-1, ^{13}C NMR spectra of compound 1 and 3, FTIR spectra of PolyA, final polymer P1, Statistical analysis of conductivity measurement and I-V plot of P1 at pH 7 and 10. Supplementary data to this article can be found online at https://doi.org/10.1016/j.eurpolymj.2022.111124.

References

[1] A. Rösler, G.W.M. Vandermeulen, H. Anton Klok, Advanced drug delivery devices via self-assembly of amphiphilic block copolymers, Adv. Drug Deliv. Rev. 64 (2012) 270–279, https://doi.org/10.1016/j.addr.2012.09.026.
[2] J.C. Brendel, F.H. Schacher, Block Copolymer Self-Assembly in Solution-Quo Vadis? Chem. Asian J. 13 (2018) 230–239, https://doi.org/10.1002/asia.201701542.
[3] M. Karayianni, S. Pispas, Block copolymer solution self-assembly: Recent advances, emerging trends, and applications, J. Polym. Sci. 59 (2021) 1874–1898, https://doi.org/10.1002/pol.20210430.
[4] Y. Mai, A. Eisenberg, Self-assembly of block copolymers, Chem. Soc. Rev. 41 (2012) 5969–5985, https://doi.org/10.1039/C2CS35115C.
[5] H. Feng, X. Lu, W. Wang, N.-G. Kang, J.W. Mays, Block Copolymers: Synthesis, Self-Assembly, and Applications, Polymers 9 (2017) 494, https://doi.org/10.3390/polym9100494.
[6] G.I. Peterson, S. Yang, T.-L. Choi, Direct formation of nano-objects via in situ self-assembly of conjugated polymers, Polym. Chem. 12 (10) (2021) 1393–1403, https://doi.org/10.1039/D0PY01389G.
[7] D.H. Lee, J.H. Lee, H.J. Kim, S. Choi, G.E. Park, M.J. Cho, D.H. Choi, (D)n–s–(A)m type partially conjugated block copolymer and its performance in singlecomponent polymer solar cells†, J. Mater. Chem. A 5 (2017) 9745–9751, https://doi.org/10.1039/C7TA01819C.
[8] C.-C. Jao, J.-R. Chang, C.-Y. Ya, W.-C. Chen, C.-J. Cho, J.-H. Lin, Y.-C. Chiu, Y. Zhou, C.-C. Kuo, Novel stretchable light-emitting diodes based on conjugated-rod block elastic-coil copolymers, Polym. Int. 70 (2021) 426–431, https://doi.org/10.1002/pi.6023.
[9] L.-L. Xiao, X. Zhou, K. Yue, Z.-H. Guo, Synthesis and Self-Assembly of Conjugated Block Copolymers, Polymers 13 (2021) 110, https://doi.org/10.3390/polym13010110.
[10] L.T. Strover, J. Malmström, J. Travas-Sejdic, Graft Copolymers with Conducting Polymer Backbones: A Versatile Route to Functional Materials, Chem. Rec. 16 (2016) 393–418, https://doi.org/10.1002/tcr.201500216.
[11] S. Maione, G. Fabregat, L.J. del Valle, A.-D. Bendrea, L. Cianga, I. Cianga, F. Estrany, C. Alemán, Effect of the graft ratio on the properties of polythiophene-g-poly(ethylene glycol), J. Polym. Sci., Part B: Polym. Phys. 53 (4) (2015) 239–252, https://doi.org/10.1002/polb.23617.
[12] E.W.C. Chan, P. Baek, D. Barker, J. Travas-Sejdic, Highly functionalisable polythiophene phenylenes, Polym. Chem. 6 (43) (2015) 7618–7629, https://doi.org/10.1039/C5PY01033K.
[13] E.H. Kwon, Y.J. Jang, G.W. Kim, M. Kim, Y.D. Park, Highly crystalline and uniform conjugated polymer thin films by a water-based biphasic dip-coating technique minimizing the use of halogenated solvents for transistor applications, RSC Adv. 9 (11) (2019) 6356–6362, https://doi.org/10.1039/C8RA09231A.
[14] Q. Tao, Y. Xia, X. Xu, S. Hedström, O. Bäcke, D.I. James, P. Persson, E. Olsson, O. Inganäs, L. Hou, W. Zhu, E. Wang, D-A1–D–A2 Copolymers with Extended Donor Segments for Efficient Polymer Solar Cells, Macromolecules 48 (4) (2015) 1009–1016, https://doi.org/10.1021/ma502186g.
[15] A. Shit, A.K. Nandi, Interface engineering of hybrid perovskite solar cells with poly (3-thiophene acetic acid) under ambient conditions†, PCCP 18 (15) (2016) 10182–10190, https://doi.org/10.1039/C6CP00502K.
[16] T. Ahn, H. Lee, S.-H. Han, Effect of annealing of polythiophene derivative for polymer light-emitting diodes, Appl. Phys. Lett. 80 (3) (2002) 392–394, https://doi.org/10.1063/1.1429292.
[17] D.T. McQuade, A.E. Pullen, T.M. Swager, Conjugated Polymer-Based Chemical Sensors, Chem. Rev. 100 (7) (2000) 2537–2574, https://doi.org/10.1021/cr9801014.
[18] S. Das, D.P. Chatterjee, S. Samanta, A.K. Nandi, Thermo and pH responsive water soluble polythiophene graft copolymer showing logic operation and nitroaromatic sensing†, RSC Adv. 3 (2013) 17540–17550, https://doi.org/10.1039/C3RA42479K.
[19] S. Das, D.P. Chatterjee, R. Ghosh, A.K. Nandi, Water soluble polythiophenes: preparation and applications, RSC Adv.. 5 (26) (2015) 20160–20177, https://doi.org/10.1039/C4RA16496B.
[20] C.D. Grande, M.C. Tria, G. Jiang, R. Ponnapati, R. Advincula, Surface-Grafted Polymers from Electropolymerized Polythiophene RAFT Agent, Macromolecules 44 (4) (2011) 966–975, https://doi.org/10.1021/ma102065u.
[21] C.-H. Lin, C.-M. Chau, J.-T. Lee, Synthesis and characterization of polythiophene grafted with a nitroxide radical polymer via atom transfer radical polymerization, Polym. Chem.. 3 (2012) 1467–1474, https://doi.org/10.1039/C2PY20048A.
[22] R. Ghosh, S. Das, D.P. Chatterjee, A.K. Nandi, Surfactant-Triggered Fluorescence Turn "on/off" Behavior of a Polythiophene-graft-Polyampholyte, Langmuir 32 (33) (2016) 8413–8423, https://doi.org/10.1021/acs.langmuir.6b0192810.1021/acs.langmuir.6b01928.s001.
[23] S. Das, S. Samanta, D.P. Chatterjee, A.K. Nandi, Thermosensitive water-soluble poly(ethylene glycol)-based polythiophene graft copolymers, J. Polym. Sci., Part A: Polym. Chem.. 51 (6) (2013) 1417–1427, https://doi.org/10.1002/pola.26514.
[24] A.D. Bendrea, G. Fabregat, J. Torras, S. Maione, L. Cianga, L.J. Del Valle, I. Cianga, C. Alemán, Polythiophene-g-poly(ethylene glycol) graft copolymers for electroactive scaffolds, J. Mater. Chem. B 1 (2013) 4135–4145, https://doi.org/10.1039/C3TB20679C.
[25] B.G. Molina, A.D. Bendrea, L. Cianga, E. Armelin, L.J. del Valle, I. Cianga, C. Alemán, The biocompatible polythiophene-g-polycaprolactone copolymer as an efficient dopamine sensor platform, Polym. Chem. 8 (39) (2017) 6112–6122, https://doi.org/10.1039/C7PY01326D.
[26] B.G. Molina, L. Cianga, A.-D. Bendrea, I. Cianga, C. Alemán, E. Armelin, An amphiphilic, heterografted polythiophene copolymer containing biocompatible/biodegradable side chains for use as an (electro)active surface in biomedical applications†, Polym. Chem. 10 (36) (2019) 5010–5022, https://doi.org/10.1039/C9PY00926D.
[27] M. Wei, Y. Gao, X. Li, M.J. Serpe, Stimuli-responsive polymers and their applications, Polym. Chem. 8 (1) (2017) 127–143, https://doi.org/10.1039/C6PY01585A.
[28] A.B. Skicki, Towards a new class of stimuli-responsive polymer-based materials – Recent advances and challenges, Appl. Surface Sci. Adv. 4 (2021) 100068, https://doi.org/10.1016/j.apsadv.2021.100068.
[29] P. Theato, B.S. Sumerlin, R.K. O'Reilly, T.H. Epps III, Stimuli responsive materials, Chem. Soc. Rev. 42 (2013) 7055–7056, https://doi.org/10.1039/C3CS90057F.
[30] N. Deirram, C. Zhang, S.S. Kermaniyan, A.P.R. Johnston, G.K. Such, pH-Responsive Polymer Nanoparticles for Drug Delivery, Macromol. Rapid Commun. 40 (2019) 1800917, https://doi.org/10.1002/marc.201800917.
[31] G. Kocak, C. Tuncer, V. Bütün, pH-Responsive polymers, Polym. Chem. 8 (1) (2017) 144–176, https://doi.org/10.1039/C6PY01872F.
[32] K. Skupov, A. Adronov, Effect of carbon nanotube incorporation into polythiophene-fullerene-based organic solar cells, Can. J. Chem. 92 (1) (2014) 68–75, https://doi.org/10.1139/cjc-2013-0460.
[33] Y.J. Lee, S.H. Kim, H. Yang, M.i. Jang, S.S. Hwang, H.S. Lee, K.-Y. Baek, Vertical Conducting Nanodomains Self-Assembled from Poly(3-hexyl thiophene)-Based Diblock Copolymer Thin Films, J. Phys. Chem. C 115 (10) (2011) 4228–4234.
[34] V. Ho, B.W. Boudouris, B.L. McCulloch, C.G. Shuttle, M. Burkhardt, M.L. Chabinyc, R.A. Segalman, Poly(3-alkylthiophene) Diblock Copolymers with Ordered Microstructures and Continuous Semiconducting Pathways, J. Am. Chem. Soc. 133 (2011) 9270–9273.
[35] X. Pang, L. Zhao, M. Akinc, J.K. Kim, Z. Lin, Novel Amphiphilic Multi-Arm, Star-Like Block Copolymers as Unimolecular Micelles, Macromolecules 44 (10) (2011) 3746–3752, https://doi.org/10.1021/ma200594j.
[36] X. Chen, B. Gholamkhass, X.u. Han, G. Vamvounis, S. Holdcroft, Polythiophene-*graft*-Styrene and Polythiophene-*graft*-(Styrene-*graft*-C_{60}) Copolymers, Macromol. Rapid Commun. 28 (17) (2007) 1792–1797, https://doi.org/10.1002/marc.200700292.
[37] I. Margalith, C. Suter, B. Ballmer, P. Schwarz, C. Tiberi, T. Sonati, J. Falsig, S. Nyström, P. Hammarström, A. Åslund, K.P.R. Nilsson, A. Yam, E. Whitters, S. Hornemann, A. Aguzzi, Polythiophenes Inhibit Prion Propagation by Stabilizing Prion Protein (PrP) Aggregates, J. Biol. Chem. 287 (23) (2012) 18872–18887, https://doi.org/10.1074/jbc.M112.355958.
[38] V.K. Tiwari, B.B. Mishra, K.B. Mishra, N. Mishra, A.S. Singh, X.i. Chen, Cu-Catalyzed Click Reaction in Carbohydrate Chemistry, Chem. Rev. 116 (5) (2016) 3086–3240, https://doi.org/10.1021/acs.chemrev.5b00408.
[39] D.S. Dissanayake, E. Sheina, M.C. Biewer, R.D. McCullough, M.C. Stefan, Determination of absolute molecular weight of regioregular poly(3-hexylthiophene) by 1H-NMR analysis, J. Polym. Sci. Part A Polym. Chem. 55 (2017) 79–82, https://doi.org/10.1002/pola.28354.
[40] M.A. Ansari, S. Mohiuddin, F. Kandemirli, M.I. Malik, Synthesis and characterization of poly(3-hexylthiophene): improvement of regioregularity and energy band gap, RSC Adv. 8 (2018) 8319–8328, https://doi.org/10.1039/C8RA00555A.
[41] V. Saini, O. Abdulrazzaq, S. Bourdo, E. Dervishi, A. Petre, V.G. Bairi, T. Mustafa, L. Schnackenberg, T. Viswanathan, A.S. Biris, Structural and optoelectronic properties of P3HT-graphene composites prepared by in situ oxidative polymerization, J. Appl. Phys. 112 (5) (2012) 054327, https://doi.org/10.1063/1.4751271.
[42] S. Hazra, A. Shit, R. Ghosh, K. Basu, A. Banerjee, A.K. Nandi, Modulation of the optoelectronic properties of a donor–acceptor conjugate between a cationic polythiophene and a peptide appended perylene bisimide ampiphile†, J. Mater. Chem. C 8 (11) (2020) 3748–3757, https://doi.org/10.1039/C9TC06593H.
[43] X. Qiao, X. Wang, Z. Mo, The $FeCl_3$-doped poly(3-alkyithiophenes) in solid state, Synth. Met. 122 (2001) 449.

[44] T.D. McCarley, Noble C.J. Dubois, R.L. McCarley, MALDI-MS Evaluation of Poly(3-hexylthiophene) Synthesized by Chemical Oxidation with $FeCl_3$, Macromolecules 34 (2001) 7999–8004, https://doi.org/10.1021/ma002140z.
[45] J.W. Onorato, C.K. Luscombe, Morphological effects on polymeric mixed ionic/electronic conductors, Mol. Syst. Des. Eng. 4 (2019) 310–324, https://doi.org/10.1039/C8ME00093J.
[46] Z. Xue, D. He, X. Xie, Poly(ethylene oxide)-based electrolytes for lithium-ion batteries, J. Mater. Chem. A 3 (2015) 19218–19253, https://doi.org/10.1039/C5TA03471J.
[47] I. Reiss, Solid State Ionics 136–137 (2000) 1119–1130, https://doi.org/10.1016/S0167-2738(00)00607-X.
[48] P. Mukherjee, A. Dawn, A.K. Nandi, Biomolecular Hybrid of Poly(3-thiophene acetic acid) and Double Stranded DNA: Optical and Conductivity Properties, Langmuir 26 (13) (2010) 11025–11034, https://doi.org/10.1021/la101215v.
[49] A. Malti, J. Edberg, H. Granberg, Z.U. Khan, J.W. Andreasen, X. Liu, D. Zhao, H. Zhang, Y. Yao, J.W. Brill, I. Engquist, M. Fahlman, L. Wågberg, X. Crispin, M. Berggren, An Organic Mixed Ion-Electron Conductor for Power Electronics Adv, Sci. 3 (2) (2016) 1500305, https://doi.org/10.1002/advs.201500305.
[50] B.D. Paulsen, K. Tybrandt, E. Stavrinidou, J. Rivnay, Organic mixed ionic–electronic conductors, Nat. Mater. 19 (1) (2020) 13–26, https://doi.org/10.1038/s41563-019-0435-z.
[51] J. Rivnay, S. Inal, A. Salleo, R.M. Owens, M. Berggren, G.G. Malliaras, Organic electrochemical transistors, Nat. Rev. Mater. 3 (2018) 17086, https://doi.org/10.1038/natrevmats.2017.86.
[52] P.P. Kumar, S. Yashonath, Ionic conduction in the solid state, J. Chem. Sci. 118 (2006) 135–154, https://doi.org/10.1007/BF02708775.